Journal of Inorganic and General Chemistry
ZAAC
Zeitschrift für anorganische und allgemeine Chemie
DOI: 10.1002/zaac.201800467
ARTICLE

Porous Gd^{III}-Organic Framework as a Dual-Functional Material for Cyanosilylation of Aldehydes and Ablation of Human Liver Cancer Cells

Dong Han,[a] Xiu-Li Yan,[a] and Jian Liu*[a]

Abstract. Metal-organic frameworks (MOFs) have gained great attention in recent years because they could behave as multifunctional materials which combine the advances of porous solids and coordination complexes. With the aim of constructing multifunctional MOFs, in this study, we choose a Y-shaped tricarboxylic ligand biphenyl-3,4′,5-tricarboxylic acid (H_3bpt) to react with Gd^{III} ions to afford a new dual-functional lanthanide-organic framework with the chemical formula of $[Gd_2(bpt)_2(H_2O)_2]\cdot(DMF)_2(H_2O)_6$ (**1**) (DMF = *N*,*N*-dimethylformamide) under solvothermal condition. The title complex was characterized by means of elemental analysis, FT-IR spectroscopy, thermogravimetric and X-ray diffraction analyses. Crystal structure analysis reveals that compound **1** is composed of 1D helical chain secondary building units that connect by the bpt^{3-} ligands into a 3D framework with 1D nanosized channels running along the *b* axis. In view of its high porosity and accessible open metal sites, the activated **1** (**1a**) was studied for the cyanosilylation of aldehydes under solvent-free conditions. The catalytic activity of **1a** is much higher than that of compound **1**, indicating that the exposed open metal sites of **1a** is beneficial to the cyanosilylation reaction. In connection to these, the different cytotoxicities of **1** and **1a** were also evaluated on four human liver cancer cells (SMMC-7721, Bel-7402, MHCC97 and Hep3B) by the MTT assay.

1 Introduction

As an important raw material, cyanohydrins have been widely used as versatile building blocks for pharmaceuticals, agrochemicals, and fine chemicals.[1] Generally, the addition of cyanide to carbonyl compounds is one of the most useful approaches for the preparation of cyanohydrins and has frequently been at the forefront of synthetic chemistry.[2] Trimethylsilyl cyanide (TMSCN) is one of the most useful and safe cyanating reagents for nucleophilic addition to carbonyl compounds to give cyanohydrin trimethylsilyl ethers.[3] Hence, the development of efficient catalysts for cyanosilylation of carbonyl compounds with TMSCN is a very important subject in current research, and several efficient catalysts have been developed so far. During the past few decades, a lot of organic catalysts have been developed for the cyanosilylation of carbonyl compounds with TMSCN, but these catalysts suffer from some drawbacks such as tedious separation and recycle problems, which restrict their practical applications.[4–6] Thus there is a great need for the developing efficient and environmental friendly catalysts for cyanohydrin reaction.

As an emerging class of crystalline material that composed of metal modes and organic connectors, metal-organic frameworks (MOFs) have gained great interests for their wide range of potential applications as functional materials in gas storage/separation, energy conversion, contamination enrichment, and so on.[7–10] In particular, MOFs have been widely studied as size- and shape-selective heterogeneous catalysts due to their large pore size, high BET surface areas and diverse functionalizations.[11–15] The removal of the coordinated solvents on the metal ion/cluster could generate the coordinatively unsaturated sites, which can be used as the activators in many organic reactions similar to the Lewis acid catalysts. Since the first discovery by *Fujita* et al., lots of papers concerning the MOFs-based catalysts for cyanosilylation have been reported.[16–18] For instance, *Kaskel* and co-workers have revealed that MIL-101-Cr is an efficient catalyst for the cyanosilylation of benzaldehyde after the removal of the coordinated water molecules.[17]

On the other hand, MOFs have also show great promise in the field of biomedicine because it has been reported that MOFs can interact with DNA through noncovalent interactions, including intercalation and groove binding for large molecules and slot external electrostatic binding for cations.[19–22] For instance, *Guo* and co-works have successfully prepared a lanthanide MOF, which shows high cytotoxicity toward the human lung cancer cell A549; *Mukherjee* and co-works have reported that the have studied the cytotoxic activity of the nanostructured MOFs on human colorectal carcinoma cell lines, and found that some of them could significantly lead to the cancer cell death. Although there are many MOFs have been shown to be capable of catalyzing cyanosilylation or inhibiting human cancer cells, none of them can achieve the above mentioned two functions simultaneously.

In this study, a new dual-functional lanthanide metal-organic framework with the chemical formula $[Gd_2(bpt)_2(H_2O)_2]\cdot(DMF)_2(H_2O)_6$ (**1**) (DMF = *N*,*N*-dimethylformamide) based on

* Dr. J. Liu
E-Mail: jian_liu666@163.com
[a] Department of Anesthesiology
Shanxian Central Hospital (Affiliated Lake West Hospital of Jining Medical College)
Shanxian, Shangdong, P. R. China
Supporting information for this article is available on the WWW under **http://dx.doi.org/10.1002/zaac.201800467** or from the author.

a Y-shaped tricarboxylic ligand biphenyl-3,4′,5-tricarboxylic acid (H_3bpt) was synthesized under solvothermal condition. The title compound was characterized by elemental analysis, FT-IR spectroscopy, thermogravimetric and X-ray diffraction analyses. Crystal structure analysis reveals that compound **1** is composed of 1D helical secondary building unit that connect by the bpt^{3-} ligands into a 3D framework with 1D nanosized channels running along the *b* axis. Furthermore, the activated **1** (**1a**) shows excellent heterogeneous catalytic activities towards the cyanosilylation of aldehydes under solvent-free conditions. The catalytic activity of **1a** is much higher than that of compound **1**, indicating that the exposed open metal sites in **1a** is beneficial to the cyanosilylation reaction. In addition, the anticancer activates of **1** were evaluated on four human liver cancer cells (SMMC-7721, Bel-7402, MHCC97 and Hep3B) by the MTT assay.

2 Experimental Section

2.1 Materials and Instrumentation

All reagents and solvents employed in this work were commercially available and used without further purification. Elemental analyses (C, H and N) were determined with Perkin–Elmer 240 elemental analyzer. Thermogravimetric analysis was carried out with a NETSCHZ STA–449C thermo-analyzer with a heating rate of 1 K·min^{-1} in a nitrogen atmosphere. Infrared spectra were measured with a Nicolet Magna 750 FT-IR spectrometer in the range of 400–4000 cm^{-1} using the KBr pellets. Powder X-ray diffraction (PXRD) analyses were recorded with a Bruker AXS D8 advanced automated diffractometer with Cu-K_α radiation.

2.2 Synthesis of $[Gd_2(bpt)_2(H_2O)_2]\cdot(DMF)_2(H_2O)_6$ (1)

A mixture of Gd_2O_3 (0.05 mmol, 0.018 g), H_3bpt (0.2 mmol, 0.058 g), DMF (4 mL), H_2O (1 mL) and three drops of concentrated nitric acid was sealed in a 20 mL glass vial. Subsequently, the mixture was heated to 90 °C and kept at that temperature for 3 d. After cooling slowly to room temperature, colorless block crystals were isolated with 45% yield based on Gd_2O_3. $C_{36}H_{44}Gd_2N_2O_{22}$: calcd. C 36.92; H 3.79; N 2.39%; found: C 36.91; N 3.42; H 2.74%. **IR** (KBr): $\tilde{\nu}$ = 3438 (w), 2978 (w), 1691 (s), 1624 (s), 1587 (s), 1476 (s), 1392 (s), 1276 (s), 1221 (s), 1108 (m), 1061 (w), 942 (w), 845 (s), 782 (m), 716 (w), 672 (m), 578 (w) cm^{-1}.

2.3 X-ray Crystallography

Single crystal X-ray crystal data of **1** was collected with a computer-controlled Oxford Xcalibu E diffractometer with graphite-monochromated Mo-K_α radiation (λ = 0.71073 Å) at room temperature. Absorption corrections were applied using SADABS. The structures were solved by direct methods by the SHELXS-2014 package and refined by full-matrix least-square methods on F^2 by using the SHELXL-2014/6. All non-hydrogen atoms were refined anisotropically and all hydrogen atoms were generated in their ideal locations. Crystallographic data and refinement details are summarized in Table 1. The selected bond lengths and angles for compound **1** are given in Table S1 (Supporting Information). The hydrogen bond details are listed in the Table S2 (Supporting Information).

Table 1. Crystal data and structure refinements for $[Gd_2(bpt)_2(H_2O)_2]\cdot(DMF)_2(H_2O)_6$ (**1**).

	1
Empirical formula	$C_{30}H_{18}Gd_2O_{14}$
Formula weight	916.94
Temperature/K	288.0(3)
Crystal system	orthorhombic
Space group	$P2_12_12$
a /Å	28.3269(2)
b /Å	14.3386(6)
c /Å	14.9223(2)
α /°	90
β /°	90
γ /°	90
Volume /Å^3	6061.0(3)
Z	4
$\rho_{calcd.}$ /g·cm^{-3}	1.005
μ /mm^{-1}	2.205
Reflections collected	16648
Independent reflections	10036 [R_{int} = 0.0362, R_{sigma} = 0.0658]
Data/restraints/parameters	10036/139/421
Goodness-of-fit on F^2	1.063
Final *R* indexes [$I \geq 2\sigma$ (*I*)]	R_1 = 0.0539, wR_2 = 0.1582
Final *R* indexes [all data]	R_1 = 0.0582, wR_2 = 0.1641
Largest diff. peak/hole /e·Å^{-3}	2.51/–2.27
Flack parameter	0.145(13)

2.4 Catalytic Test for Cyanosylation Reaction

A suspension of an aromatic aldehyde (1.0 mmol), trimethylsilyl cyanide (TMSCN, 2.0 mmol) and catalyst (2.5 mol%, compounds **1** or **1a**) was placed in a Schlenk tube in an nitrogen atmosphere. Afterwards, the mixture was stirred at 50 °C under solvent-free conditions until disappearance of the aldehydes (0.25–4 h, checked by GC-MS). The catalyst was removed by centrifugation and filtered quickly with ethyl acetate. The conversion of aldehydes was determined by gas chromatography (GC, Agilent 7890A) analysis.

2.5 MTT Assay

The anticancer activity of compounds **1**, **1a**, and the drug Vinorebine was evaluated against four human liver cancer cells (SMMC-7721, Bel-7402, MHCC97 and Hep3B) via the MTT assay. The two cancer cell lines were seeded in a 96-well plate, in which the cells density is 5000 cells per test well, and cultured overnight at 37 °C in a 5% CO_2 incubator. The tested compounds were dispersed in DMSO and diluted in the respective medium containing 1% fetal bovine serum (FBS). After 24 h, the medium was replaced with the respective medium with 1% FBS containing the compound **1** at various concentrations. After 48 h, 10 μL of MTT (5 mg/mL) in phosphate buffered saline (PBS) was added to each well and incubated at 37°C for 4 h. The medium with MTT was then flicked off, and the formed formazan crystals were dissolved in 100 μL of DMSO. The absorbance was measured at 570 nm with a microplate reader. The percentage of cell inhibition was determined using the formula, %inhibition = [mean OD of untreated cells (control)/mean OD of treated cells (control)] × 100 and a graph was plotted with the percentage of cell inhibition vs. concentration. From this, the IC_{50} value was calculated.

Crystallographic data (excluding structure factors) for the structure in this paper have been deposited with the Cambridge Crystallographic Data Centre, CCDC, 12 Union Road, Cambridge CB21EZ, UK. Copies of the data can be obtained free of charge on quoting the de-

pository number CCDC-1876617 (Fax: +44-1223-336-033; E-Mail: deposit@ccdc.cam.ac.uk, http://www.ccdc.cam.ac.uk).

Supporting Information (see footnote on the first page of this article): Additional structural figures, PXRD patterns, TGA curves, N2 sorption isotherm, NMR data and the table for the selected bond lengths and angles.

3 Results and Discussion

3.1 Crystal Structure of Compound 1

Compound **1** was synthesized by reaction of Gd_2O_3 and H_3bpt in a mixed solvent of DMF and H_2O with the presence of HNO_3. It should be noted that only white deposition was obtained without the presence of HNO_3, indicating the HNO_3 might act as a pH regulator which is very important for the formation of the water soluble Gd^{3+} ions in the reaction process. Single crystal X-ray diffraction analysis revealed that compound **1** crystallizes in orthorhombic $P2_12_12$ space group and features a 3D framework based on the 1D helical chain secondary building unit. The asymmetric unit of **1** is composed of two crystallographically independent Gd^{III} ion, two bpt^{3-} ligands, and two coordinated water molecules. As shown in Figure 1a, both Gd1 and Gd2 atoms show the similar seven-coordinated surroundings that are finished by seven O atoms (eight carboxylic O atoms for Gd1, two water O atoms, and five carboxylic O atoms for Gd2).

The coordination arrangement of the two Gd^{III} ions could be best described as a pentagonal bipyramid as calculated with the SHAPE software. The Gd^{III}–O bond lengths range from 2.258(5) Å to 2.414(5) Å, which locate in the normal range among the Gd^{III}–O bond lengths of the reported Gd^{III}-carboxylate MOFs in the literature.[9] Gd1 and Gd2 atoms are held together by the carboxylic groups of the bpt^{3-} ligand to afford a dinuclear unit with the Gd1–Gd2 separation of 5.906(3) Å, which is further extended into a 1D right-handed helical secondary building unit chain via the bpt^{3-} ligand along the *b* axis (Figure 1b). As for the bpt^{3-} ligand, they reveal two different coordination modes: one binds with five Gd ions using its three carboxylic groups showing the μ_2-η^1:η^1, μ_2-η^1:η^1, and μ_1-η^1:η^1 fashion; the other one connects with six different Gd ions using its three carboxylic groups showing the same μ_2-η^1:η^1 pattern. The connection of the 1D helical SBUs with the bpt^{3-} ligands generates a porous three-dimensional framework with 1D rhombus channels running along the *b* axis. The window size for the 1D channel is 11.3×8.6 Å^2, which fills with water occupied open metal sites (Figure 1c).

The coordination water molecule forms hydrogen bonding interaction with the carboxylic O atom and the donor-acceptor distance is 1.891 Å (O13–H13···O2, Figure S1, Supporting Information). With omitting the coordinated water molecules, PLATON analysis revealed that the 3D framework is composed of voids of 3928.8 Å^3, which represent 64.8 % per unit cell volume. TOPOS software was used to simplify this framework. In this 3D framework, the two Gd ions could be treated as 5 and 6-connected node, and the one and two half bpt^{3-} ligands could be considered as 5, 6 and 6-connected nodes, so the whole framework of **1** could be viewed as a

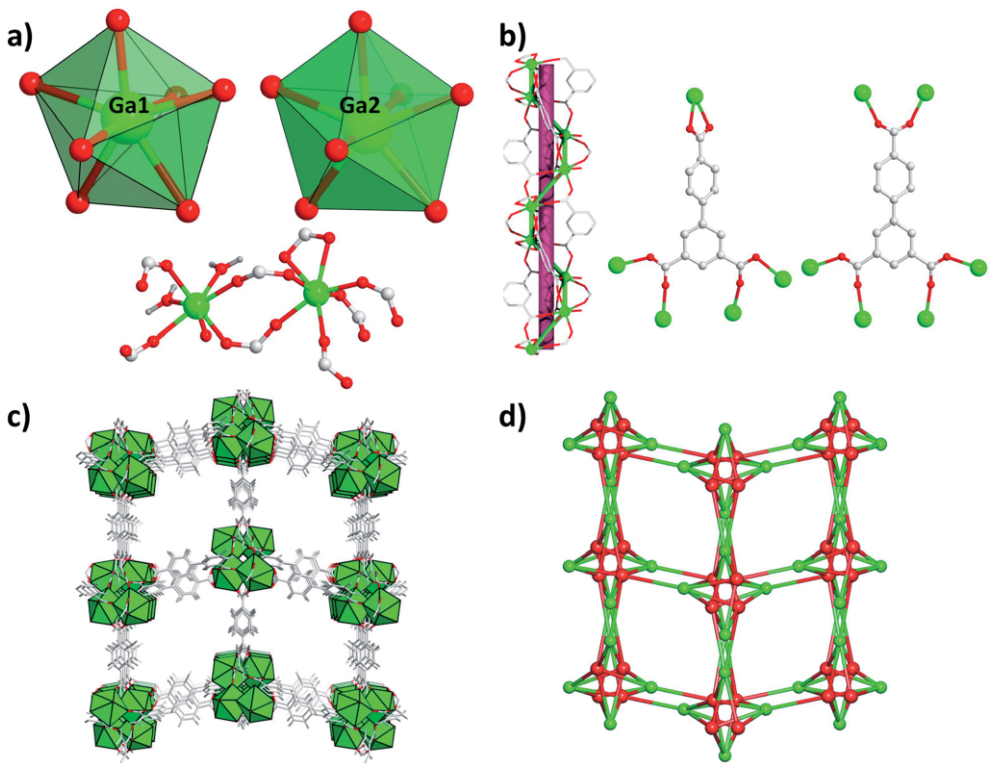

Figure 1. (a) View of the coordination environments of Gd^{III} ions in **1**. (b) The 1D helical SBUs and the coordination modes of the organic ligand. (c) The 3D framework of compound **1**. (d) The schematic representation of the simplified topological network for compound **1**.

5,5,6,6,6-connected net with a point symbol of {4^5.6^5}{4^8.6^7}{4^9.6^5.8}{4^9.6} (Figure 1d).

3.2 PXRD and Thermogravimetric Analysis for Compound 1

The simulated and experimental PXRD patterns of **1** are shown in Figure S2a (Supporting Information). Their peak positions are in good agreement with each other, indicating the phase purity of the products. In addition, the thermal stability of **1** was also analyzed on crystalline samples from 30–800 °C in a nitrogen atmosphere (Figure S2b). The TGA curve of **1** shows that it experienced a three-step weight loss process. The first weight loss of 9.18 % (calcd. 9.24 %) occurred in the temperature range of 53–100 °C, which can be attributed to the departure of the free water molecules. The second weight loss of 15.32 % (calcd. 15.57 %) occurred in the temperature range of 130–180 °C that corresponds to the loss of the coordinated water and lattice DMF molecules. After taking off the solvent molecules, the framework of **1** is stable up to 300 °C, which was also confirmed by the powder X-ray diffraction of the activated samples (Figure S2a). Upon heating above 300 °C, the skeleton of **1** begins to collapse with the third weight loss.

The permanent porosity of the activated **1** (**1a**) was unambiguously established by its N_2 sorption isotherm at 77 K. The activated sample **1a** was prepared by exchanging the solvent and it was characterized by PXRD measurement, indicating that the framework was maintained because the broadened peaks positions remained (Figure S2a). The N_2 adsorption study at 77 K of **1** reveals type I nitrogen adsorption isotherm with the maximum uptake capacity of 316 $cm^3 \cdot g^{-1}$, suggesting that **1a** mainly contain microporous cavities (Figure S3, Supporting Information). The calculated Brunauer–Emmett–Teller (BET) and Langmuir surface areas of **1a** are 985 and 1124 $m^2 \cdot g^{-1}$, respectively. Using the Horvath–Kawazoe (HK) method on the N_2 sorption isotherms, pore size distribution was estimated, which reveals a pore size location of 8.6 Å, and thus is basically identical to the results from the single-crystal X-ray diffraction study.

3.3 Catalytic Activity

To evaluate the catalytic activity of compounds **1** and **1a**, we used the cyanosilylation of carbonyl compounds catalyzed by Lewis acids as a test reaction (Scheme 1). The reaction of carbonyls with trimethylsilyl cyanide (TMSCN) in the presence of a catalyst produces the corresponding cyanohydrin trimethylsilyl ethers, which are industrially valuable and important intermediates. The cyanosilylation was carried out in the presence of **1a** with a 1:2 molar ratio of the selected carbonyls and TMSCN at room temperature in a nitrogen atmosphere. The conversions were calculated based on GC and the results are summarized in Table 2. Using compound **1** as the catalyst, the conversion of benzaldehyde and its derivatives can reach above 58.85–78.57 % in 2 h. Using **1a** as the catalysts, the conversion of benzaldehyde and its derivatives can reach above 95–99 % under the same conditions.

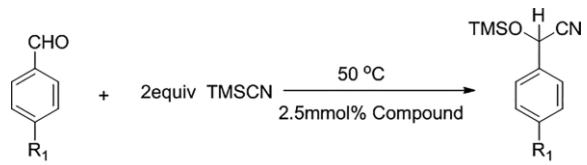

R1=H, F, Me, t-Bu, 1-Naphthyl

Scheme 1. The cyanosilylation reaction in the presence of selected complexes.

The cyanosilylation yield of **1a** is much higher than that of many MOFs used for the cyanosilylation study under the similar conditions, which might be ascribed to its large inner spaces and high density of exposed metal sites.[23–26] It is noteworthy that the catalytic activity of **1a** is higher than that of compound **1**. This can be attributed to more open metal sites of Gd^{3+} in **1a**, which can effective enhance the catalytic activity. The stability of compound **1a** was examined after the catalytic study by PXRD, which reveals the same PXRD pattern as the as-synthesized phase, indicating that the compound was stable. In addition, the parallel experiment without

Table 2. The results for the catalytic cyanosilylation of aldehydes in the presence of **1** and **1a**.

Aldehyde	Blank /% [a]	**1** conversion /% [a]	**1a** conversion /% [a]
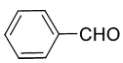	12.36	76.13	99.32
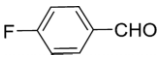	16.59	78.57	99.58
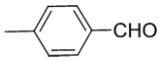	13.22	69.15	99.47
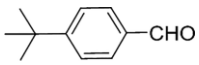	10.36	58.85	95.43
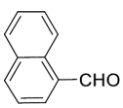	6.82	18.34	24.25

a) Conversion determined by GC; the NMR spectra for the products are shown in Figure S4 (Supporting Information).

Table 3. Growth inhibitory effects on SMMC-7721, Bel-7402, MHCC97, and Hep3B cells.

Compound	IC_{50} /μM SMMC-7721	Bel-7402	MHCC97	Hep3B
1	>100	>100	>100	>100
1a	25	25	35	40
H_3bpt	>100	>100	>100	>100
$Gd(NO_3)_3{\cdot}6H_2O$	>100	>100	>100	>100
Vinorebine	35	25	30	45

catalyst was also done, the conversion of benzaldehyde and its derivative is below 20 %. These results indicate that compound **1a** can be used as efficient catalysts for the cyanosilylation reaction under mild conditions. To further explore whether the activation of the carbonyl species occurs inside the pores or on the surface of the solid catalyst, substrates of increasing dimensions were tested, a significant size-selectivity effect is observed with catalyst, when the substrate was 1-naphthaldehyde with dimensions 9.7×8.4 Å^2, the conversion was reduced to 24.25 % for **1a**.

Based on the experimental results and previously reported results, a plausible reaction mechanism is proposed to illustrate the process of **1**' catalyzed cyanosilylation reaction.[23,24] The labile water molecules in the channels of compound **1** were removed by heating to expose the unsaturated metal sites previously. The aldehydes were activated by the coordinatively unsaturated central Ga atoms to react with TMSCN (Scheme 2). The products were replaced by aldehydes, and the catalysts were continued to activate the aldehydes in the next catalytic cycle.

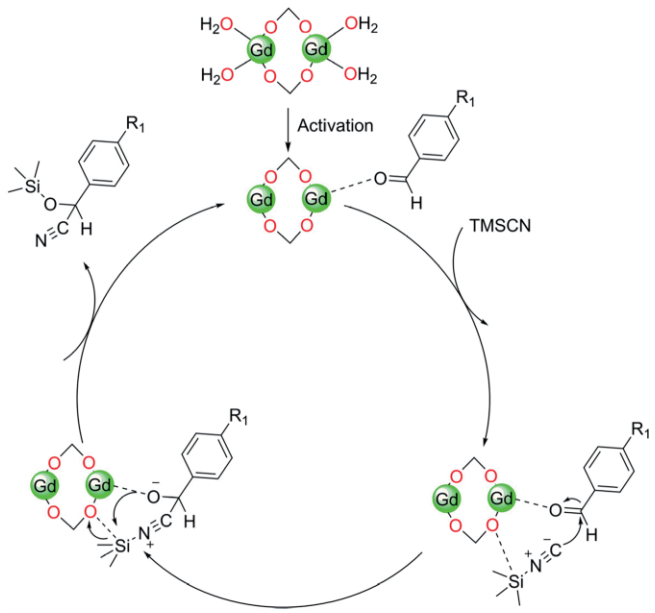

Scheme 2. Proposed mechanism for the cyanosilylation reaction of carbonyl compounds catalyzed by **1a**.

3.4 Antitumor Activity

The interesting structural features and the obviously different of complexes **1** and **1a** encouraged us to test their cytotoxicity against a panel of human liver cancer cells (SMMC-7721, Bel-7402, MHCC97, and Hep3B) and by MTT (3-(4,5-dimethylthiazol-2-yl)-2,5-diphenyltetrazolium bromide) assay method. Compounds were dissolved in DMSO and blank samples containing the same volume of DMSO were taken as controls to identify the activity of solvent in this cytotoxicity experiment. The reference drug Vinorebine was used as a positive control to assess the cytotoxicity of the test compounds. The results were analyzed by means of cell inhibition expressed as IC_{50} values and they are summarized in Table 3. It is obvious that compound **1** is inactive against all of these cell lines ($IC_{50} > 100$ μM). At this concentration, it should exert high cytotoxicity against these cells, so we concluded that it exerted no inhabitation selectivity towards these cell lines. However, after the tumor cells were incubated in the presence of compound **1a** for 72 h, the IC_{50} value ranged from 25 to 40 μM, some of which were even lower than those of Vinorebine, indicating that compound **1a** exhibited antitumor activity against all of these cell lines in different degrees. It is to be noted that the ligand and $Gd(NO_3)_3{\cdot}6H_2O$ did not show any significant activity on all the four cancer cells (IC_{50} = above 700–900 μM), which confirmed that the chelation of the ligand with the open Gd^{III} sites is the only responsible factor for the observed cytotoxic properties of complex **1a**. The better cytotoxic activity of **1a** than that of complex **1** may be attributed to the extended planar structure induced by the π–π* conjugation resulting from the removal of the coordinated water molecules on the Gd^{III} sites, which make them interact with the DNA more easily and finally leads to the cell death.

4 Conclusions

A new porous Gd^{III}-organic framework based on a Y-shaped tricarboxylic ligand biphenyl-3,4′,5-tricarboxylic acid (H_3bpt) was synthesized under solvothermal condition. Crystal structure analysis reveals that compound **1** is composed of 1D helical chain secondary building unit that connects by the bpt^{3-} ligands into a 3D framework with 1D nanosized channels. The activated **1** could be used as a dual-functional material for effective cyanosilylation of aldehydes under solvent-free conditions and inhibition of human cancer cell growth. These findings clearly indicate that the MOFs may behave as multifunctional materials by choosing suitable building blocks. The information obtained from our study would be helpful to understand the mechanism of cyanosylation reaction in MOFs as well as the interactions of ligand bridged Gd^{III} complexes with DNA and should be useful in the development of better materials for substrate-dependent cyanosylation reaction and new therapeutic agents for certain diseases.

Keywords: d^{III} compound; Biphenyl-3,4′,5-tricarboxylic acid; Solvothermal reaction; Cyanosilylation reaction; Gadolinium; MTT assay

References

[1] R. J. H. Gregory, *Chem. Rev.* **1999**, *99*, 3649–3682.
[2] E. J. Corey, W. Zhe, *Tetrahedron Lett.* **1993**, *34*, 4001–4004.
[3] L. Romero-Hernández, *Synlett* **2015**, *26*, 563–564.
[4] B. Karimi, L. Ma'Mani, *Org. Lett.* **2004**, *6*, 4813–4815.
[5] Y. Kikukawa, K. Suzuki, M. Sugawa, T. Hirano, K. Kamata, K. Yamaguchi, N. Mizuno, *Angew. Chem. Int. Ed.* **2012**, *51*, 3686–3690.
[6] J. J. Song, F. Gallou, J. T. Reeves, Z. Tan, N. K. Yee, C. H. Senanayake, *J. Org. Chem.* **2006**, *71*, 1273–1276.
[7] D. Liu, T. F. Liu, Y. P. Chen, L. Zou, D. Feng, K. Wang, Q. Zhang, S. Yuan, C. Zhong, H. C. Zhou, *J. Am. Chem. Soc.* **2015**, *137*, 7740–7746.
[8] D. Chen, W. Shi, P. Cheng, *Chem. Commun.* **2015**, *51*, 370–372.
[9] J. P. Ma, S. Q. Wang, C. W. Zhao, Y. Yu, Y. B. Dong, *Chem. Mater.* **2015**, *27*, 3805–3808.
[10] J. S. Qin, D. Y. Du, W. Guan, X. J. Bo, Y. F. Li, L. P. Guo, Z. M. Su, Y. Y. Wang, Y. Q. Lan, H. C. Zhou, *J. Am. Chem. Soc.* **2015**, *137*, 7169–7177.
[11] J. Liang, Y. B. Huang, R. Cao, *Coord. Chem. Rev.* **2017**, *358*, 92–107.
[12] R. Babu, A. C. Kathalikkattil, R. Roshan, J. Tharun, D. W. Kim, D. W. Park, *Green Chem.* **2016**, *18*, 232–242.
[13] S. Wu, L. Chen, B. Yin, Y. Li, *Chem. Commun.* **2015**, *51*, 9884–9887.
[14] Y. Feng, H. Fan, Z. Zhong, H. Wang, D. Qiu, *Inorg. Chem.* **2016**, *55*, 11987–11992.
[15] Y. Feng, M. Li, H. Fan, Q. Huang, D. Qiu, H. Shi, *Dalton Trans.* **2015**, *44*, 894–897.
[16] C. W. Duan, L. X. Hu, J. L. Ma, *J. Mater. Chem. A* **2018**, *6*, 6309–6318.
[17] A. Henschel, K. Gedrich, R. Kraehnert, S. Kaskel, *Chem. Commun.* **2008**, *15*, 4192–4194.
[18] L. M. Aguirre-Díaz, M. Iglesias, N. Snejko, E. Gutiérrez-Puebla, M. Á. Monge, *RSC Adv.* **2015**, *5*, 7058–7065.
[19] K. Wang, X. Ma, D. Shao, Z. Geng, Z. Zhang, Z. Wang, *Cryst. Growth Des.* **2012**, *12*, 3786–3791.
[20] D. S. Raja, N. S. P. Bhuvanesh, K. Natarajan, *Dalton Trans.* **2012**, *41*, 4365–4377.
[21] M. Y. Guo, X. Zhang, L. Zhao, Y. K. Li, D. Y. Chen, G. W. Yang, Q. Y. Li, *J. Solid State Chem.* **2018**, *259*, 104–109.
[22] S. Mukherjee, S. Ganguly, K. Manna, S. Mondal, S. Mahapatra, D. Das, *Inorg. Chem.* **2018**, *57*, 4050–4060.
[23] A. Karmakar, S. Hazra, M. F. C. Guedes da Silva, A. J. L. Pombeiro, *Dalton Trans.* **2015**, *44*, 268–280.
[24] L. M. Aguirre-Díaz, M. Iglesias, N. Snejko, E. Gutiérrez-Puebla, M. Á. Monge, *CrystEngComm* **2013**, *15*, 9562–9571.
[25] S. Neogi, M. K. Sharma, P. K. Bharadwaj, *J. Mol. Catal. A* **2009**, *299*, 1–4.
[26] A. Bhunia, S. Dey, J. M. Moreno, U. Diaz, P. Concepcion, K. Van Hecke, C. Janiak, P. Van Der Voort, *Chem. Commun.* **2016**, *52*, 1401–1404.

Received: November 2, 2018
Published online: January 15, 2019

